SWEDISH DEFENCE
RESEARCH AGENCY

FOI-R--0140--SE
June 2001
ISSN 1650-1942

Base data report

Andreas Helte, Eric Lillberg

A comparison of potential and viscous flow models for pressure signature computations

Weapons and Protection
SE-147 25 Tumba

SWEDISH DEFENCE RESEARCH AGENCY

Weapons and Protection
SE-147 25 Tumba

FOI-R--0140--SE

June 2001

ISSN 1650-1942

Base data report

Andreas Helte, Eric Lillberg

A comparison of potential and viscous flow models for pressure signature computations

Issuing organization FOI – Swedish Defence Research Agency Weapons and Protection SE-147 25 Tumba	**Report number, ISRN** FOI-R--0140--SE	**Report type** Base data report
	Research area code 5. Combat	
	Month year June 2001	**Project no.** E2009
	Customers code 1. Research for the Government	
	Sub area code 52 Underwater Weapons	
Author/s (editor/s) Andreas Helte Eric Lillberg	**Project manager** Paul Ström	
	Approved by	
	Scientifically and technically responsible	

Report title

A comparison of potential and viscous flow models for pressure signature computations

Abstract (not more than 200 words)

The pressure field and surface wave pattern generated by a submerged sphere advancing at constant speed in calm water have been calculated by two different methods. The first method uses the Navier-Stokes equations coupled with the Volume of Fluid method to treat the free surface. The second method uses a potential flow model with a linearized free surface condition. Good agreement is found for the calculated wave pattern close to the sphere, but the results diverges further away. Due to large fluctuations from the turbulent flow field in the calculated pressure using the viscous solver, a comparison for the calculated pressure is difficult to make.

Keywords

Pressure signatures, potential flow, Navier-Stokes, free surface, surface waves

Further bibliographic information	**Language** English
ISSN 1650-1942	**Pages** 10 p.
	Price acc. to pricelist
	Security classification

Utgivare Totalförsvarets Forskningsinstitut - FOI Vapen och skydd 147 25 Tumba	**Rapportnummer, ISRN** FOI-R--0140--SE	**Klassificering** Underlagsrapport
	Forskningsområde 5. Bekämpning	
	Månad, år Juni 2001	**Projektnummer** E2009
	Verksamhetsgren 1. Forskning för regeringens behov	
	Delområde 52 Undervattensvapen	
Författare/redaktör Andreas Helte Eric Lillberg	**Projektledare** Paul Ström	
	Godkänd av	
	Tekniskt och/eller vetenskapligt ansvarig	
Rapportens titel (i översättning) Jämförelse mellan potentialströmning och viskös modell för beräkning av trycksignaturer		
Sammanfattning (högst 200 ord) En jämförande studie av två metoder för beräkning av tryckfält och ytvågor från en sfär med konstant hastighet under en fri vattenyta har utförts. De båda metoderna baseras på potentialströmnings teori med ett lineariserat randvillkor på ytan samt Navier-Stokes ekvationer med Volume of Fluid metoden för att hantera vattenytan. Beräkningarna av ytvågorna visar god överensstämmelse mellan de båda metoderna nära sfären, medan våghöjden skiljer avsevärt mellan modellerna längre nedströms. För den viskösa Navier-Stokes lösningen är trycksignaturen på botten svår att urskilja i tryckfältet från det turbulenta strömningsfältet.		
Nyckelord Trycksignaturer, potentialströmning, Navier-Stokes, fri vätskeyta, ytvågor		
Övriga bibliografiska uppgifter	**Språk** Engelska	
ISSN 1650-1942	**Antal sidor:** 10 s.	
Distribution enligt missiv	**Pris: Enligt prislista** **Sekretess**	

Contents

1 Introduction

Pressure sensitive sea mines reacts on the depression generated by a passing vessel. To design trigger criterions for sea mines or construct mine sweepers, it is important to be able to calculate how the depression depends on the vessel hull design, speed and sea depth.

In general, the most accurate computational methods include the effects from viscous dissipation and surface tension and are based on the full Navier-Stokes equations coupled with a free surface condition. This system of equations is usually solved using a finite element, finite volume or finite difference method. If viscous effects are of less or no importance, a potential flow model can be used. In potential flow the velocity is assumed to have a scalar potential, which satisfies Laplace equation. A tractable method for solving Laplace equation is the Boundary Integral Method, BIM, in which the potential is expressed as a convolution surface integral of a kernel (the Greens function) and the potential over the enclosed boundary. The free surface condition on the water surface, which is not known in advance, is in general non-linear. An iterative method is thus required to find a water surface consistent with the boundary condition for the potential on the water surface. Furthermore, the surface integral over the water surface must be extended far enough to eliminate influence from artificial boundaries. If the hull is entirely submerged, the free surface can be linearized around the undisturbed water surface. By using a Greens function that satisfies the linearized free surface condition, the complications mentioned above can be avoided.

In the present study the wave pattern, pressure signature and flow field around a submerged sphere advancing at constant speed on calm water is considered. A comparison is made between two different approaches, a potential flow model and a viscous flow model, to compute the free surface waves and pressure signature resulting from the motion the sphere. The potential flow model is solved with a linearized free surface condition. The viscous model adopted here is the Navier-Stokes equations with gravitational forces acting on the fluid together with the Volume of Fluid method, VOF. In VOF the free surface is represented by a transported scalar field representing the volume fraction of water to air in the computational volume. The effective density of the fluid is then averaged using the volume fraction in each computational cell. The system of equations is solved using a finite volume method.

In section 2 we give a brief description of the two methods used in the present study for computing the flow field around the submerged sphere. In section 3 we present some computational results for the pressure field and the wave pattern using the two methods. The choice of a submerged body was dictated by the inability of the potential flow solver in its present form to treat surface ships. In section 4 we summarize the results and comments on discrepancies between the computed values and discusses the advantages and disadvantages with each method.

2 Computational models

2.1 Problem assumptions and definitions

We consider a sphere traveling at constant speed u_0 in calm water. The sea bottom is assumed rigid and is located at the constant depth h. The water is considered incompressible with the density ρ and the acceleration of gravity is denoted by g. We choose a coordinate system moving with the vessel with the propagation direction along the negative x-axis and the z-axis directed upward. Above the water surface the pressure has the constant value p_{atm}.

2.2 Potential flow model with linearized free surface boundary condition

In the potential flow model the fluid is assumed to be inviscid and the flow irrotational. In this case the flow velocity has a scalar potential, $\mathbf{u} = u_0\mathbf{e}_x + \nabla\phi$, which satisfies the Laplace equation

$$\nabla^2\phi = 0. \quad (1)$$

From Bernoulli's law the pressure can be expressed as

$$p = p_0 - \rho(u_0\phi_x + \phi_t + \tfrac{1}{2}|\nabla\phi|^2), \quad (2)$$

where $p_0 = p_{\text{atm}} - \rho g z$ is the hydrostatic pressure. If the water surface is defined by $z = \eta(x,y)$ and the surface tension is neglected, the requirement that the pressure at the water surface equals the air pressure gives an equation for the wave elevation,

$$\eta = -(u_0\phi_x + \phi_t + \tfrac{1}{2}|\nabla\phi|^2)/g, \quad (3)$$

which is augment by the kinematic condition

$$\partial_t\eta(x,y,t) + \mathbf{u}\cdot\nabla(\eta(x,y,t) - z) = 0. \quad (4)$$

If the body is fully submerged, the perturbation velocity at the water surface is small compared to the inflow velocity. If terms quadratic in the perturbation velocity are neglected, a linearized boundary condition on the unperturbed surface $z = 0$ is obtained as

$$\begin{cases} \eta = -(u_0\phi_x + \phi_t)/g \\ -(u_0\eta_x + \eta_t) + \phi_z = 0 \end{cases}. \quad (5)$$

Eliminating η from these equations gives the linearized free surface condition

$$\left(\frac{\partial}{\partial x} + \frac{1}{u_0}\frac{\partial}{\partial t}\right)^2\phi + \nu\phi_z = 0, \quad (6)$$

where $\nu = g/u_0^{\ 2}$. The Laplace equation (1) with boundary condition (6) can be rewritten as a boundary integral equation for the perturbation potential on the hull H,

$$-\tfrac{1}{2}\phi(\mathbf{r}') + \int_H \phi(\mathbf{r})G_n(\mathbf{r},\mathbf{r}')dS = -u_0\int_H n_x G(\mathbf{r},\mathbf{r}')dS, \quad \mathbf{r}\in H, \quad (7)$$

where $G(\mathbf{r},\mathbf{r}')$ is the Greens function for the Laplace operator which satisfies the linearized free surface condition (6) and the sea bottom condition $G_z(\mathbf{r},\mathbf{r}')$ at $z = -h$. A detailed discussion of the computation of the free surface Greens function and the numerical method used for solving the boundary integral equation is given in reference [1].

2.3 Viscous flow model

For the viscous solution we solve the Navier-Stokes equations together with transport equation for a scalar field representing the volume fraction of water in a computational cell. This method is termed Volume of Fluid and is widely used in flow computations where two different fluids coexist and where the interfaces are not explicitly defined. Hence, the density ρ is averaged over a control volume using the volume fraction α and the densities of the two fluids. The indicator function α takes the value 1 in the water and 0 in the air, and satisfies a Lagrange invariant. In mathematical terms the system of equations becomes,

$$\begin{cases} \operatorname{div} \mathbf{u} = 0, \\ \partial_t(\mathbf{u}) + \operatorname{div}(\mathbf{u} \otimes \mathbf{u}) = -\operatorname{grad} p + \operatorname{div} \mathbf{S} + \rho \mathbf{g} + \mathbf{f}, \\ \partial_t(\alpha) + \operatorname{div}(\alpha \mathbf{u}) = 0, \end{cases} \quad (8)$$

where **u** is the velocity vector, $\rho = \alpha\rho_1 + (1-\alpha)\rho_2$ is the density, $\mathbf{S} = 2\mu\mathbf{D}$ the viscous stress tensor, $\mu = \alpha\mu_1 + (1-\alpha)\mu_2$ the viscosity, with indices referring to water as fluid 1 and air as fluid 2, and **f** the surface tension. Surface tension is a tensile force tangential to the interface separating the fluids with its magnitude depending mainly on the nature of the fluids. For wavelengths on the meter scale, however, the surface tension can usually be neglected. The definition of the indicator function implies that α is a step function and thus ρ is discontinuous. In order to model the two fluids as a continuum by using (8_3), ρ should be continuous and differentiable over the domain, [2]. To accomplish this we give the transitional region between the two fluids a small but finite thickness d, i.e. α=1 in fluid 1, α=0 in fluid 2 and 0<α<1 within the transitional region. To capture the dynamics of the thin interface separating water and air a particular reconstruction algorithm, the Compressive Interface Capturing Scheme for Arbitrary Meshes (CICSAM), for the convection term in the α-equation is used. Further details of the used CICSAM scheme is given by Ubbink, [3].

The system of equations (8) is not solved for directly, as in Direct Numerical Simulations, DNS, but filtered in space using the mesh size, resulting in the Large Eddy Simulation, LES, model. LES has emerged as a promising alternative to the Reynolds Averaged Navier-Stokes, RANS, model in order to confront the scale-complexity problem inherent to high Re-number flows. In RANS the NS are averaged in time, dividing the velocity into mean and fluctuating parts, resulting in a model most suitable for stationary applications. In LES the motion is separated into small and large scale eddies (eddies being the most appropriate fluid mechanical components to consider) and equations are solved for the latter.

3 Results for the excess pressure and wave pattern generated by a submerged sphere

To compare the quality of the two different models, the excess pressure at the sea bottom and the wave elevation generated by a submerged sphere were computed with the two methods. The radius of the sphere was set to 0.5 meters, the total depth 4 meters, the forward velocity 2 m/s and the distance from the sphere center to the unperturbed water surface 1 m. For the potential flow model, no exterior boundaries are necessary to introduce. For the NS-solver the computational domain was extended 4 m upstream and 10 m downstream. The channel width was 8 m. At the inlet boundary $\mathbf{u} = u_0\mathbf{e}_x$ and $\nabla p \cdot \mathbf{e}_x = 0$. At the outlet boundary $p = p_0$ and $\partial\, \mathbf{u} / \partial\, x = 0 \cdot$

The viscous solution is subject to physical dissipation phenomena as well as dissipation and dispersion through the numerics applied in the discretisation process. These effects becomes evident when comparing the wave cuts from the two models along lines parallel to the direction of flow at different distances from the symmetry plane, see figures 1. Compared with the non-viscous solution, the wave elevation is in good agreement close to the sphere but decreased significantly faster in the viscous solution further downstream. It should be noted that the LES model produces a time accurate solution. Hence, the solution and wave elevation changes significantly over time. A remedy to this problem is time averaging of the surface elevation but this was not made in the present study.

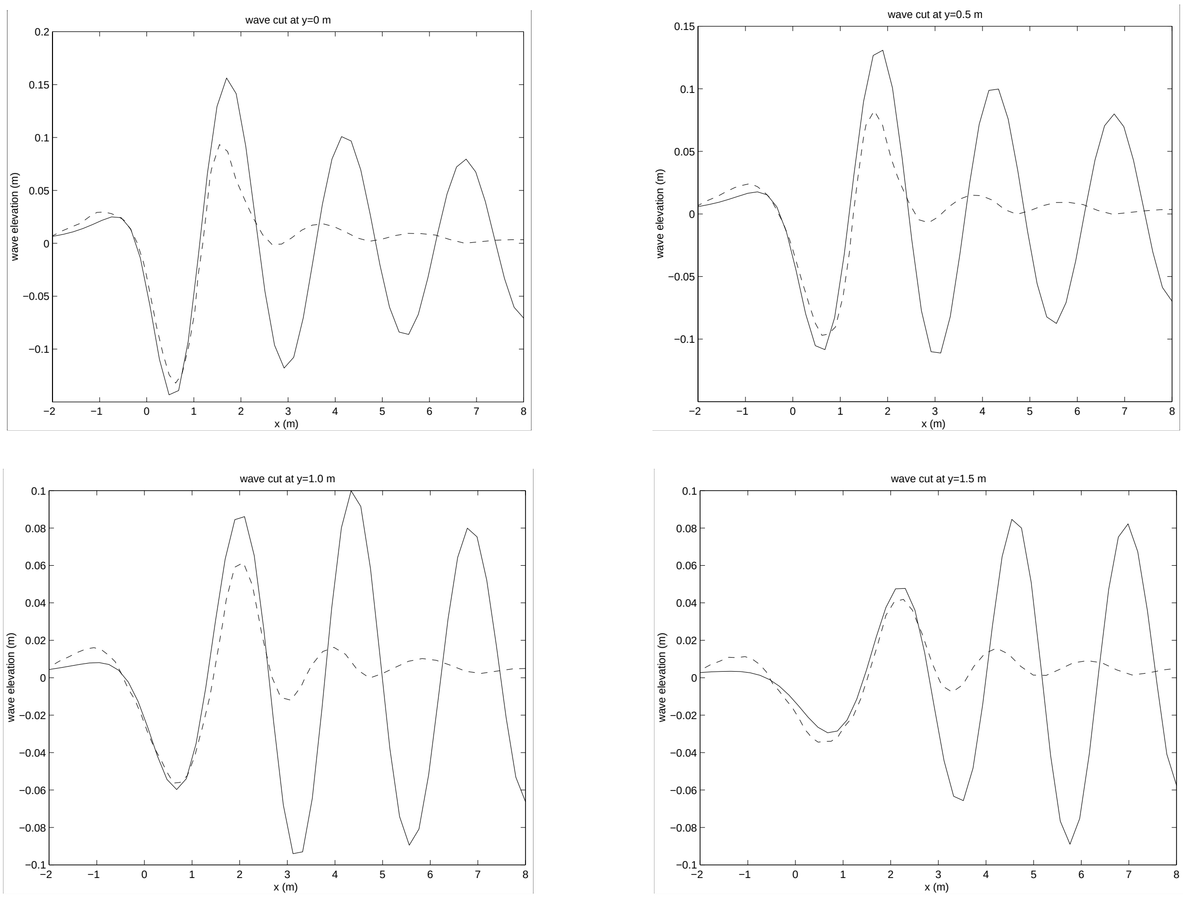

Figure 1: The computed wave elevation along four different cuts in the *y*-axis. Solid lines are from the potential flow solver and dotted lines are from the NS-solver.

In figure 2 the free surface elevation is shown for both models. The wave pattern predicted by the two models has the same character but differs in amplitude. Also the shape differs slightly where the viscous solution has a wider crest, perpendicular to the direction of flow, than the non-viscous model.

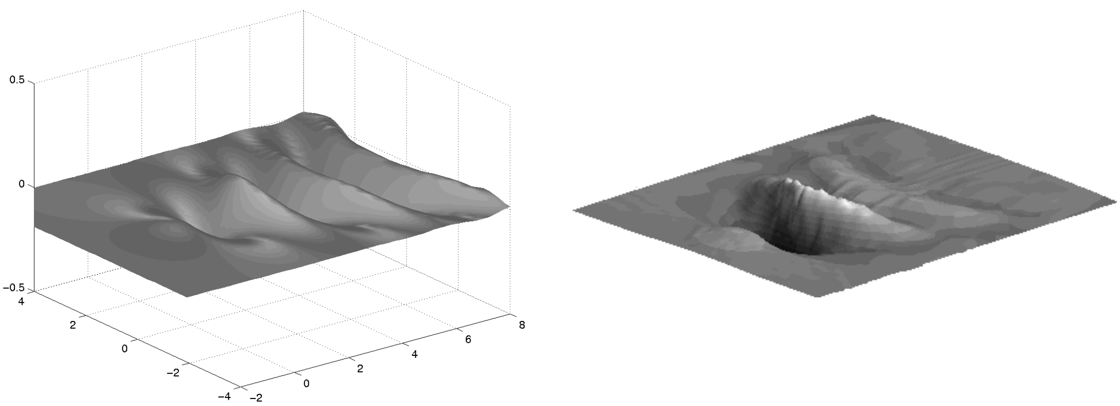

Figure 2: Surface wave pattern on the water surface.

In figure 3 contours of the pressure distribution at the bottom, z = 4 m, is shown for both solutions. The hydrostatic pressure has been subtracted to show the pressure change due to the motion of the sphere. It shows a significant pressure drop under the sphere of about –25 Pa for both the potential flow model and the Navier-Stokes solution. The excess pressure at the bottom predicted by the viscous model, at this speed, is too small to easily be distinguished from the random pressure fluctuations in the turbulent flow field. Again, a remedy to this problem, as for the surface elevation, is time averaging.

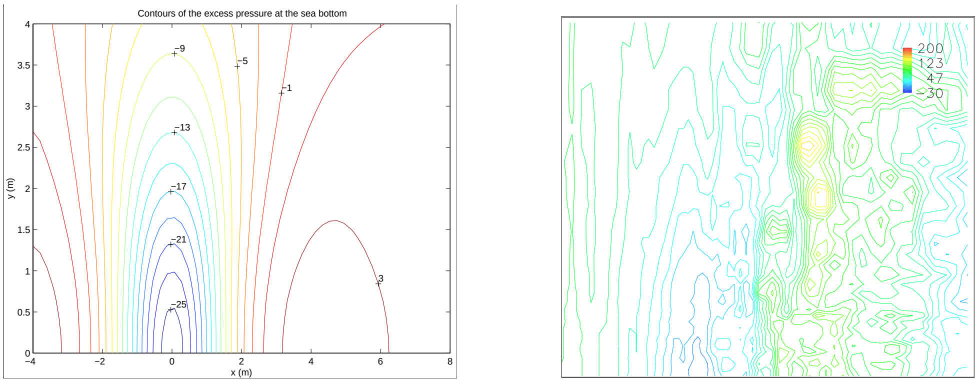

Figure 3: Contours of the pressure distribution at z = 4 m. Non-viscous solution (left) and viscous solution (right)

In figure 4 the turbulent wake behind the sphere in the viscous solution is shown. An isosurface of the magnitude of the vorticity vector colored with its component in the direction of flow reveals a thick swirling tail of intense vorticity downstream of the sphere. Also shown in figure 4 is the free surface colored with the x-component of the vorticity vector showing the vortical structures responsible for some of the physical dissipation of the surface waves.

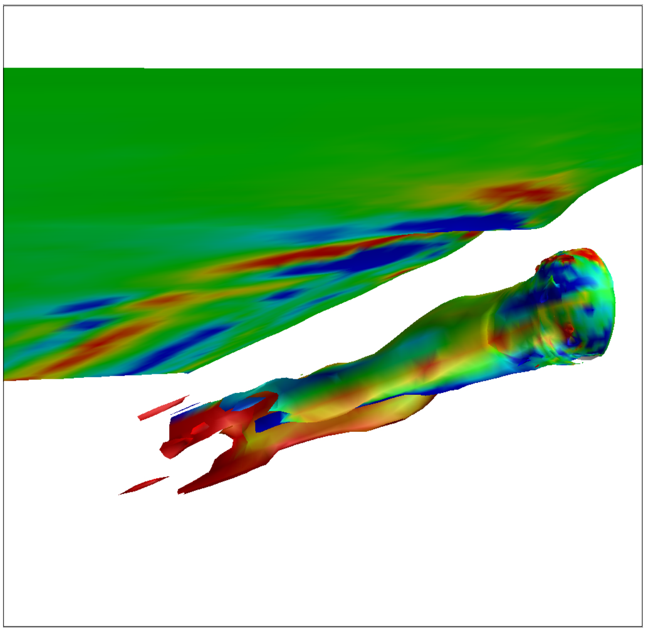

Figure 4: Perspective view from below showing the free surface and an isosurface of the vorticity magnitude, both colored with the streamvise component of the vorticity vector.

4 Conclusions

In the present study a comparison has been made between two different methods for computing the wave patter and pressure field generated by a submerged sphere. A non-viscous method was used based on a potential flow model with a linearized free surface condition. Also, a viscous method based on the Navier-Stokes equations together with a volume of fluid method was used. The computed results show good agreement for the wave patterns close to the sphere but the viscous model has a greater damping of the wave elevation further downstream. This is likely caused by the lack of viscous forces in the potential flow model or by the numerical dissipation and dispersion through the numerics applied in the discretisation. Also, the boundary conditions used for the viscous solver have some damping influence on the free surface elevation.

Regarding the pressure distribution computed with the viscous method there are some difficulties in resolving the small amplitude pressure distribution resulting from the sphere in the fluctuating pressure from the turbulent flow field. However, the computed minimum pressure is of the same magnitude for both models.

Both methods applied in this study have their benefits and drawbacks. The non-viscous method used in this study cannot handle surface ships due to the linearized surface condition and also neglects viscous effects. However, the method does not suffer from artificial boundaries conditions and computationally inexpensive. Also, the pressure distribution is easily computed. On the other hand, the viscous solution depends on initial and boundary conditions that introduces errors in the computation, especially close to the boundaries. Also, the numerical dissipation and dispersion acts deteriorating on the free surface waves. Its benefits are the ability to give a more physical and detailed flow field in general, and to add the viscous effects to the problem in particular, since these are important close to the sphere.

In conclusion it is found that LES is too computationally expensive to use in a domain large enough for the effects of the boundary conditions to be negliable. If only the pressure distribution at the bottom is of interest, than a potential flow model with non-linear surface conditions, or possibly a RANS model, is more appropriate. However, the best solution would be a combination of the LES model, for near field calculations, with a potential flow model for the far field. In this case the linearized surface condition used in this study can be applied.

References

[1] A. Helte.; 2000, ”Beräkning av tryckfältet kring en undervattensfarkost med en randintegralmetod”. FOA-R--00-01726-313--SE.

[2] Sussman M., Smereka P. & Osher S.; 1994, “A Level-set Approach for Computing Solutions to Incompressible Two-Phase Flows”, J. Comp. Phys., **114**, p 146.

[3] Ubbink O.; 1997, “Numerical Prediction of Two Fluid Systems with Sharp Interfaces”, PhD Thesis, London University.